

How imperfect interfaces affect the nonlinear transport properties in composite nanomaterials

Fabio Pavanello and Stefano Giordano

Citation: *J. Appl. Phys.* **113**, 154310 (2013); doi: 10.1063/1.4801889

View online: <http://dx.doi.org/10.1063/1.4801889>

View Table of Contents: <http://jap.aip.org/resource/1/JAPIAU/v113/i15>

Published by the [American Institute of Physics](#).

Additional information on J. Appl. Phys.

Journal Homepage: <http://jap.aip.org/>

Journal Information: http://jap.aip.org/about/about_the_journal

Top downloads: http://jap.aip.org/features/most_downloaded

Information for Authors: <http://jap.aip.org/authors>

ADVERTISEMENT



AIP Advances

Now Indexed in
Thomson Reuters
Databases

Explore AIP's open access journal:

- Rapid publication
- Article-level metrics
- Post-publication rating and commenting

How imperfect interfaces affect the nonlinear transport properties in composite nanomaterials

Fabio Pavanello¹ and Stefano Giordano^{2,a)}

¹IEMN, UMR CNRS 8520, Avenue Poincaré, BP 60069, 59652 Villeneuve d'Ascq, France

²International Associated Laboratory LEMAC/LICS: IEMN, UMR CNRS 8520, PRES Lille Nord de France, ECLille, Avenue Poincaré, BP 60069, 59652 Villeneuve d'Ascq, France

(Received 11 February 2013; accepted 1 April 2013; published online 17 April 2013)

Nanomaterials composed of a population of particles dispersed in a matrix represent the building block for the next generation of several technologies: energy storage and conversion, thermal management, electronics, and photovoltaics. When interfaces between particles and matrix are imperfect, the size of the particles may strongly influence the effective linear and nonlinear response of the whole system. Here, we study these scale effects mainly focussing on the nonlinear transport behavior of composite structures. The theory is developed, in the framework of the electrical conductivity, for an arbitrary nonlinearity of the constituents; however, explicit results are discussed for Kerr-like nonlinear responses. Two kinds of imperfect interfaces are considered: the T-model and the Π -model, which represent a generalization of the classical schemes largely employed in literature, namely the low and the high conducting interface models. The dependence of the nonlinear effective properties on the size of the dispersed particles is explained through intrinsic length scales governing some universal scaling laws. © 2013 AIP Publishing LLC
<http://dx.doi.org/10.1063/1.4801889>

I. INTRODUCTION

In modern materials science, heterogeneous structures (i.e., nanocomposites or nanoalloys) are widely investigated because of their remarkable properties of large technological interest. One of the most important problem concerns their characterization, i.e., the evaluation of their effective physical properties, measurable at a large observation scale.^{1,2} The microstructure of such heterogeneous systems typically ranges from the microscale to the nanoscale: at this level of miniaturization the nonlinearity of the constituents and the properties of their interfaces cannot be neglected and play a central role.

The first crucial aspect for understanding the behavior of nanosystems is the nonlinearity of their constitutive equations. In the context of the electrical conduction it means that the current density \vec{J} may be nonlinearly related to the local electric field \vec{E} .³ Considerable attention has been devoted to homogenization techniques for electromagnetically nonlinear composite structures.^{4–6} Such methods find applications, for instance, in the study of the intrinsic optical bistability^{7,8} and of the second and third harmonic generation.^{9,10} Populations of nonlinear ellipsoids have been considered both with random¹¹ and pseudo-random^{12,13} orientations. Moreover, dispersions of linear and nonlinear spheroidal inclusions with randomly distributed geometric factors have been studied.¹⁴ Also, results concerning dispersions of dielectrically nonlinear and graded structures have been achieved.¹⁵

The second important point concerns the complexity of the interfaces between different phases. As a matter of fact, scale effects in nanostructured materials are driven by

imperfect interfaces because of the small surface/volume ratio. The electrical potential V and the normal component of the current density \vec{J} may be discontinuous across the interface between two components: $\llbracket V \rrbracket \neq 0$ and/or $\llbracket \vec{J} \cdot \vec{n} \rrbracket \neq 0$ (where $\llbracket f \rrbracket$ represents the jump of f across the interface).³ In order to consider the effects of the interfaces two simple zero thickness models have been introduced in pioneering works. The first model is called *low conducting interface*: in this case we have $\llbracket \vec{J} \cdot \vec{n} \rrbracket = 0$, while the electrical potential suffers a jump proportional to the local flux, $\llbracket V \rrbracket = -r\vec{J} \cdot \vec{n}$, where r is the Kapitza-like resistance.¹⁶ The second model is called *high conducting interface* and concerns the case of an interphase with $\llbracket V \rrbracket = 0$ and the jump of the flux is proportional to the surface Laplacian of the electrical potential, $\llbracket \vec{J} \cdot \vec{n} \rrbracket = g\nabla_S^2 V$, where g is the interphase conductance. A large number of investigations on composite materials with low^{17–27} or high^{20,26,28–33} conducting interfaces can be found in literature. Other models are based on interphases of finite thickness described by a refined mathematical formalism.^{34–36}

In this paper, we analyze the combined effects of nonlinear phases joined through imperfect interfaces: more specifically, we determine the scale effects induced by complex interfaces on the effective nonlinear properties of a nanocomposite material. We take into consideration a paradigmatic structure composed of nonlinear circular (2D) or spherical (3D) inhomogeneities embedded in a linear matrix (see Fig. 1). The theory can be applied to an arbitrary nonlinearity of the particles. However, explicit results are discussed for a Kerr-like nonlinearity described by a field dependent conductivity of the form $\sigma_2(E_i) = \sigma_2 + \chi_2 E_i^2$. On the other hand, the interface behavior is taken into account by means of the T-model and the Π -model, which are complex interface structures recently introduced to generalize the

^{a)}Electronic mail: Stefano.Giordano@iemn.univ-lille1.fr

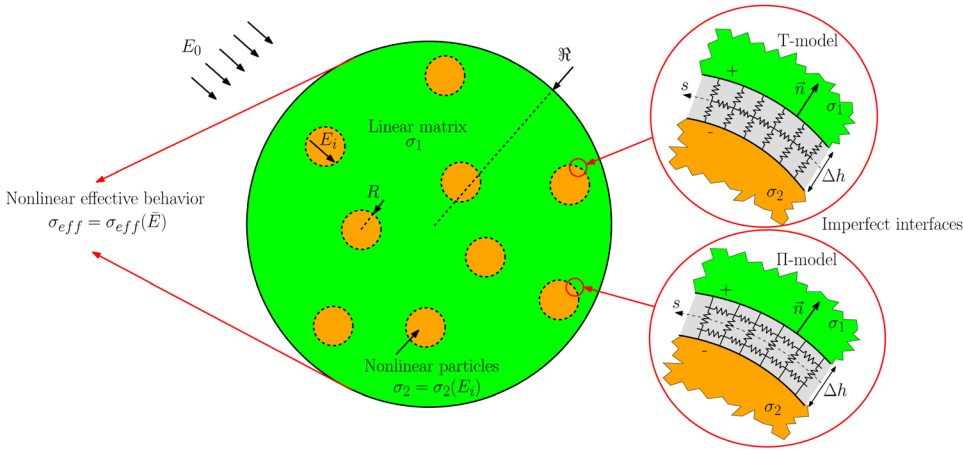


FIG. 1. Scheme of a nanostructure composed of nonlinear particles embedded in a linear matrix: the imperfect interfaces are modelled either through the T-model or the Π -model. The multiscale approach leads to evaluate the nonlinear effective behavior of the overall system.

low and high conducting interface models.³⁷ In these generalized schemes both the electrical potential and the normal component of the current density are discontinuous at the interface. The versatility of such structures allows us to effectively describe the behavior of real imperfect/multilayered/structured interfaces of broad technological interest.

At first, we adopted these interfaces to model a single particle embedded in a different matrix. The most important technique to study the inclusion/matrix configuration is the Eshelby methodology, largely employed for the electric, magnetic, thermal, and elastic case.^{38–41} Its application allowed to prove that the field induced in circular or spherical particles with low or high conducting interfaces is uniform if the externally applied field is so.^{27,32,33} For isotropic phases this property is valid also for the T and Π structures.³⁷

Previous results for a single particle are constructive for determining the nonlinear behavior of dispersions of nonlinear particles with imperfect interfaces. Indeed, we prove that the effective nonlinear properties depend upon the size of the inhomogeneities. The complete understanding of these behaviors is presented here by introducing different intrinsic length scales governing various universal scaling laws. It is important to remark that the same length scales are able to characterize both the linear and nonlinear scaling scenario.

We underline that all the achievements of the present paper can be also used in quasi-static regime if we consider a wavelength λ much larger than the radius R of the particles.

II. THE T AND Π DUAL MODELS FOR IMPERFECT INTERFACES

In order to generalize the high and low conducting interfaces, we proposed in Ref. 37 two more refined models exploiting the network topologies shown in Fig. 1. The first model is based on the T-lattice structure and it is defined by three parameters r^+ , g , and r^- , whose physical meaning is widely discussed in Ref. 37. Briefly, r^+ and r^- [$\Omega \text{ m}^2$] represent the longitudinal (along \vec{n}) external and internal resistivities of the lattice. Moreover, g [Ω^{-1}] represents the transversal (perpendicular to \vec{n}) conductivity of the lattice. In the limit of a continuous zero-thickness interphase layer ($\Delta h \rightarrow 0$), we easily obtain the relations for the interface in the form

$$[[V]] = -r^+(\vec{J} \cdot \vec{n})^+ - r^-(\vec{J} \cdot \vec{n})^-, \quad (1)$$

$$[[\vec{J} \cdot \vec{n}]] = g r^+ \frac{\partial^2}{\partial s^2} (\vec{J} \cdot \vec{n})^+ + g \frac{\partial^2}{\partial s^2} V^+. \quad (2)$$

In previous expressions, the partial derivatives are performed with respect to the variable s , which represents the curvilinear abscissa along the arbitrarily curved interface on the plane. As usual, in the three-dimensional case the operator $\partial^2/\partial s^2$ must be substituted with the surface Laplacian ∇_s^2 , which is briefly discussed in Ref. 37. We can observe that the present approach reproduces the low conducting interface model if $g=0$ (with a Kapitza resistance $r = r^- + r^+$) and the high conducting interface model if $r^- = r^+ = 0$.

A dual scheme can be introduced by considering the second structure depicted in Fig. 1 (Π -model). A procedure similar to the previous one leads to the following interface equations:

$$[[V]] = -r(\vec{J} \cdot \vec{n})^+ + r g^+ \frac{\partial^2}{\partial s^2} V^+, \quad (3)$$

$$[[\vec{J} \cdot \vec{n}]] = g^+ \frac{\partial^2}{\partial s^2} V^+ + g^- \frac{\partial^2}{\partial s^2} V^-, \quad (4)$$

where g^+ and g^- [Ω^{-1}] represent the transversal external and internal conductivities, while r [$\Omega \text{ m}^2$] represents the longitudinal resistivity of the lattice. As before, the operator $\partial^2/\partial s^2$ must be substituted with the surface Laplacian ∇_s^2 for the 3D case. The Π -model reproduces the low conducting interface model if $g^- = g^+ = 0$ and the high conducting interface model if $r = 0$.

As described in Ref. 37, both models can also be interpreted through a series of three ideal sheets, each of them being a low or a high conducting interface. Moreover, the evident structural and geometrical duality of the models will be observed also in the linear and nonlinear physical results described below.

III. BEHAVIOR OF A LINEAR PARTICLE WITH GENERALIZED INTERFACES

We consider now a single circular (in 2D) or spherical (in 3D) particle with conductivity σ_2 (linear) embedded into

a matrix with conductivity σ_1 (linear): to begin, we suppose that the interface between the constituents is described by Eqs. (1) and (2) (T-model) and we determine the effect of an externally applied field. Here, we are interested in the case of a uniform field E_0 , corresponding to a potential $V_0 = -\rho \cos \vartheta E_0$. We underline that E_0 is aligned to the x -axis when we consider a 2D geometry (with polar coordinates $x = \rho \cos \vartheta$ and $y = \rho \sin \vartheta$) and to the z -axis when we consider a 3D geometry (with spherical coordinates $x = \rho \sin \vartheta \cos \varphi$, $y = \rho \sin \vartheta \sin \varphi$, and $z = \rho \cos \vartheta$): for details see Fig. 2 of Ref. 37. The perturbation induced by the inhomogeneity with imperfect contact has been eventually found as

$$\text{for } \rho < R \Rightarrow V = -\rho \cos \vartheta E_0 \left(\frac{d\sigma_1}{C} \right), \quad (5)$$

$$\text{for } \rho > R \Rightarrow V = -\rho \cos \vartheta E_0 \left(1 + \frac{R^d \mathcal{B}}{\rho^d C} \right), \quad (6)$$

where $d=2$ for the circle and $d=3$ for the sphere; the parameters \mathcal{B} and \mathcal{C} are defined as follows:

$$\mathcal{B} = \sigma_1 - \sigma_2 + \frac{r^+ + r^-}{R} \sigma_1 \sigma_2 - (d-1) \frac{g}{R} \left[1 - r^+ \frac{\sigma_1}{R} \right] \left[1 + r^- \frac{\sigma_2}{R} \right], \quad (7)$$

$$\mathcal{C} = (d-1)\sigma_1 + \sigma_2 + (d-1) \frac{r^+ + r^-}{R} \sigma_1 \sigma_2 + (d-1) \frac{g}{R} \left[1 + (d-1)r^+ \frac{\sigma_1}{R} \right] \left[1 + r^- \frac{\sigma_2}{R} \right]. \quad (8)$$

The electric quantities both inside and outside the particle, in contrast to the case with perfect interfaces, depend on R . Indeed, these results were used for analyzing the scale effects induced by the imperfect contact.³⁷ From Eq. (5) it is easy to identify the induced internal field as $E_i = d\sigma_1 E_0 / C$. The linear scaling law for $R \rightarrow \infty$ was obtained by introducing the classical Lorentz field for a particle with a perfect interface $E_L = E_i|_{r^+ = r^- = 0, g=0}$; we easily proved that³⁷

$$\frac{E_i}{E_L} - 1 = -\frac{(d-1)\sigma_1}{(d-1)\sigma_1 + \sigma_2} \frac{\ell^- + \ell^+ + \mathcal{L}}{R} + O\left(\frac{1}{R^2}\right), \quad (9)$$

where we introduced the following intrinsic length scales:

$$\ell^- = \sigma_2 r^-, \quad \ell^+ = \sigma_2 r^+, \quad \mathcal{L} = \frac{g}{\sigma_1}, \quad (10)$$

which control all the scaling laws (also the nonlinear ones as described below). This result means that the internal field approaches the Lorentz one for large radius of the particle ($R \gg \ell^- + \ell^+ + \mathcal{L}$), i.e., the effects of the contact imperfection are vanishingly small for $R \rightarrow \infty$.

Now, we can also consider the Π -model described by Eqs. (3) and (4). The perturbation to the electric potential generated by the inhomogeneity with imperfect interface is described again by Eqs. (5) and (6), but with new coefficients \mathcal{B} and \mathcal{C} given below

$$\mathcal{B} = \sigma_1 - \sigma_2 + \frac{r}{R} \sigma_1 \sigma_2 - (d-1)^2 \frac{g^- g^+ r}{R^3} - \frac{(d-1)}{R} \left\{ g^- \left[1 - r \frac{\sigma_1}{R} \right] + g^+ \left[1 + r \frac{\sigma_2}{R} \right] \right\}, \quad (11)$$

$$\mathcal{C} = (d-1)\sigma_1 + \sigma_2 + (d-1) \frac{r}{R} \sigma_1 \sigma_2 + (d-1)^2 \frac{g^- g^+ r}{R^3} + \frac{(d-1)}{R} \left\{ g^- \left[1 + (d-1)r \frac{\sigma_1}{R} \right] + g^+ \left[1 + r \frac{\sigma_2}{R} \right] \right\}. \quad (12)$$

As before, they strongly depend on R , showing evident scale effects. With regards to the scaling law for $R \rightarrow \infty$, we proved that³⁷

$$\frac{E_i}{E_L} - 1 = -\frac{(d-1)\sigma_1}{(d-1)\sigma_1 + \sigma_2} \frac{\ell + \mathcal{L}^+ + \mathcal{L}^-}{R} + O\left(\frac{1}{R^2}\right), \quad (13)$$

where we introduced the dual intrinsic length scales

$$\ell = \sigma_2 r, \quad \mathcal{L}^+ = \frac{g^+}{\sigma_1}, \quad \mathcal{L}^- = \frac{g^-}{\sigma_1}. \quad (14)$$

As expected, also in this case the internal field approaches the Lorentz one for large radius of the particle ($R \gg \ell + \mathcal{L}^+ + \mathcal{L}^-$). In the following, we will prove that also the nonlinear features exhibit scale effects governed by the same length scales.

IV. HOMOGENIZATION OF DISPERSIONS WITH NONLINEAR PARTICLES

We take into consideration a random and isotropic dispersion of N nonlinear circular or spherical particles embedded in a linear matrix, and we suppose that the interfaces are modelled either through the T-model or the Π -model (see Fig. 1). The volume fraction of the dispersed particles is assumed to be small by hypothesis. We can therefore generalize the Maxwell approach,⁴² or equivalently, the Mori-Tanaka scheme⁴³ by obtaining the effective nonlinear behavior of the system. We suppose that $\sigma_2 = \sigma_2(E_i)$, i.e., the particles are nonlinear with an arbitrary field-dependent conductivity. Hence, the parameters \mathcal{B} and \mathcal{C} above defined become functions of the internal field E_i : $\mathcal{B} = \mathcal{B}(E_i)$ and $\mathcal{C} = \mathcal{C}(E_i)$.

To begin, we consider each single independent (i.e., non-interacting) particle and we can simply write

$$\text{for } \rho < R \Rightarrow E_i = \frac{d\sigma_1}{C(E_i)} E_0, \quad (15)$$

$$\text{for } \rho \gg R \Rightarrow V = -\rho \cos \vartheta E_0 \left[1 + N \frac{R^d \mathcal{B}(E_i)}{\rho^d C(E_i)} \right]. \quad (16)$$

The first relation represents an implicit equation for the internal field E_i induced within each particle (derived from Eq. (5)). If the value of E_i is determined (numerically or analytically), the second equation gives the electric potential far from the heterogeneous system ($\rho \gg R$), as superposition of the effects of all inhomogeneities. It is important to remark that this potential is also influenced by the nonlinear behavior of the dispersion. This point will be exploited to perform the nonlinear homogenization.

On the other hand, we can take into consideration the nonlinear homogenized circle or sphere of radius \mathfrak{R} , representing the overall heterogeneous system (see Fig. 1). It is described by a nonlinear constitutive equation $\sigma_{eff} = \sigma_{eff}(\bar{E})$ (which is unknown for the moment), where \bar{E} represents the average value of the electric field over the composite structure. Of course, the equivalent circle or sphere is embedded in a matrix of conductivity σ_1 with perfect interfaces. Therefore, we can simply write

$$\text{for } \rho < \mathfrak{R} \Rightarrow \bar{E} = \frac{d\sigma_1}{(d-1)\sigma_1 + \sigma_{eff}(\bar{E})} E_0, \quad (17)$$

for $\rho \gg \mathfrak{R} \Rightarrow$

$$V = -\rho \cos \vartheta E_0 \left[1 + \frac{\mathfrak{R}^d}{\rho^d} \frac{\sigma_1 - \sigma_{eff}(\bar{E})}{(d-1)\sigma_1 + \sigma_{eff}(\bar{E})} \right]. \quad (18)$$

While the first equation represents a direct relation between the applied field and the averaged one, the second equation furnishes the electric potential in the region far from the composite system.

We will prove that an *ad hoc* analysis of the four results given in Eqs. (15)–(18) is able to yield the effective nonlinear response of the overall heterogeneous structure. To this aim we can obtain a direct relationship between the internal field E_i and the average field \bar{E} over the whole volume by combining Eqs. (15) and (17): the result is

$$\bar{E} = \frac{E_i \mathcal{C}(E_i)}{(d-1)\sigma_1 + \sigma_{eff}(\bar{E})}. \quad (19)$$

Similarly, we can compare Eqs. (16) and (18) and we eventually obtain a second relation as follows:

$$\frac{\mathcal{B}(E_i)}{\mathcal{C}(E_i)} = \frac{1}{c} \frac{\sigma_1 - \sigma_{eff}(\bar{E})}{(d-1)\sigma_1 + \sigma_{eff}(\bar{E})}, \quad (20)$$

where we have introduced the volume fraction c defined as $c = NR^d/\mathfrak{R}^d$, N being the total number of inhomogeneities within the surface of radius \mathfrak{R} . Now, we can obtain $\sigma_{eff}(\bar{E})$ from Eq. (20) and we can substitute it in Eq. (19). Performing these calculations, we proved that Eqs. (19) and (20) are equivalent to the following expressions:

$$\bar{E} = \frac{\mathcal{C}(E_i) + c\mathcal{B}(E_i)}{d\sigma_1} E_i, \quad (21)$$

$$\sigma_{eff}(\bar{E}) = \sigma_1 \left[1 - \frac{cd\mathcal{B}(E_i)}{\mathcal{C}(E_i) + c\mathcal{B}(E_i)} \right], \quad (22)$$

which finally solve the proposed problem. From the first equation we can determine $E_i = E_i(\bar{E})$ and we can use this dependence in the second equation by obtaining $\sigma_{eff} = \sigma_{eff}(\bar{E})$, which is the searched nonlinear effective constitutive equation. This general scheme, as above anticipated, is valid for an arbitrary nonlinearity $\sigma_2 = \sigma_2(E_i)$ of the particles. Nevertheless, its implementation must be performed numerically for complex forms of the function $\sigma_2 = \sigma_2(E_i)$. Here, we are interested in analytically applying

this procedure for nonlinear particles described by a quadratic (Kerr-like) response

$$\sigma_2(E_i) = \sigma_2 + \chi_2 E_i^2. \quad (23)$$

It is worth to note that σ_2 in the right hand side is a constant coefficient, while in the left hand side it represents a function of E_i . The parameter χ_2 controls the nonlinear hyper-susceptibility of the particles. As a result, we will determine the overall nonlinear response of the nanocomposite in the form

$$\sigma_{eff}(\bar{E}) = \sigma_{eff} + \chi_{eff} \bar{E}^2 + \delta_{eff} \bar{E}^4 + O(\bar{E}^6), \quad (24)$$

where σ_{eff} is the effective linear conductivity and χ_{eff} and δ_{eff} are the effective nonlinear properties of our system. First of all we can obtain the explicit forms of the parameters $\mathcal{B} = \mathcal{B}(E_i)$ and $\mathcal{C} = \mathcal{C}(E_i)$: to do this, we combine Eq. (23) with Eqs. (7) and (8) for the T-model and with Eqs. (11) and (12) for the Π -model. In any case, we obtain

$$\mathcal{B}(E_i) = \alpha_B + \beta_B E_i^2, \quad (25)$$

$$\mathcal{C}(E_i) = \alpha_C + \beta_C E_i^2, \quad (26)$$

where for the T-model, the coefficients are given by the following expressions:

$$\alpha_B = \sigma_1 - \sigma_2 + \frac{r^+ + r^-}{R} \sigma_1 \sigma_2 - (d-1) \frac{g}{R} \left[1 - r^+ \frac{\sigma_1}{R} \right] \left[1 + r^- \frac{\sigma_2}{R} \right], \quad (27)$$

$$\alpha_C = (d-1)\sigma_1 + \sigma_2 + (d-1) \frac{r^+ + r^-}{R} \sigma_1 \sigma_2 + (d-1) \frac{g}{R} \left[1 + (d-1)r^+ \frac{\sigma_1}{R} \right] \left[1 + r^- \frac{\sigma_2}{R} \right], \quad (28)$$

$$\beta_B = -\chi_2 + \frac{r^+ + r^-}{R} \sigma_1 \chi_2 - (d-1) \frac{g}{R^2} \left[1 - r^+ \frac{\sigma_1}{R} \right] r^- \chi_2, \quad (29)$$

$$\beta_C = \chi_2 + (d-1) \frac{r^+ + r^-}{R} \sigma_1 \chi_2 + (d-1) \frac{g}{R^2} \left[1 + (d-1)r^+ \frac{\sigma_1}{R} \right] r^- \chi_2, \quad (30)$$

and for the Π -model by the following ones:

$$\alpha_B = \sigma_1 - \sigma_2 + \frac{r}{R} \sigma_1 \sigma_2 - (d-1)^2 \frac{g^- g^+ r}{R^3} - \frac{(d-1)}{R} \left\{ g^- \left[1 - r \frac{\sigma_1}{R} \right] + g^+ \left[1 + r \frac{\sigma_2}{R} \right] \right\}, \quad (31)$$

$$\alpha_C = (d-1)\sigma_1 + \sigma_2 + (d-1) \frac{r}{R} \sigma_1 \sigma_2 + (d-1)^2 \frac{g^- g^+ r}{R^3} + \frac{(d-1)}{R} \left\{ g^- \left[1 + (d-1)r \frac{\sigma_1}{R} \right] + g^+ \left[1 + r \frac{\sigma_2}{R} \right] \right\}, \quad (32)$$

$$\beta_B = -\chi_2 + \frac{r}{R} \sigma_1 \chi_2 - \frac{(d-1)}{R^2} g^+ r \chi_2, \quad (33)$$

$$\beta_C = \chi_2 + (d-1) \frac{r}{R} \sigma_1 \chi_2 + \frac{(d-1)}{R^2} g^+ r \chi_2. \quad (34)$$

The first point concerns the solution of Eq. (21) with the assumption given in Eqs. (25) and (26). Hence, we have to find E_i in terms of \bar{E} starting from

$$\bar{E} = \frac{(\alpha_C + \beta_C E_i^2) + c(\alpha_B + \beta_B E_i^2)}{d\sigma_1} E_i, \quad (35)$$

which corresponds to

$$d\sigma_1 \bar{E} = (\alpha_C + c\alpha_B)E_i + (\beta_C + c\beta_B)E_i^3. \quad (36)$$

This is an algebraic cubic equation of the form $ax + bx^3 = c$. The solution can be searched in form of series in the parameter c , by obtaining $x = \frac{c}{a} - \frac{bc^3}{a^4} + 3\frac{b^2c^5}{a^7} + O(c^7)$; therefore, the solution of Eq. (36) can be written as

$$E_i = \frac{d\sigma_1}{\alpha_C + c\alpha_B} \bar{E} - \frac{\beta_C + c\beta_B}{(\alpha_C + c\alpha_B)^4} d^3 \sigma_1^3 \bar{E}^3 + 3\frac{(\beta_C + c\beta_B)^2}{(\alpha_C + c\alpha_B)^4} d^5 \sigma_1^5 \bar{E}^5 + O(\bar{E}^7). \quad (37)$$

Now to complete the procedure we have to substitute Eq. (37) into Eq. (22); the result is given in Eq. (24) where the linear and nonlinear effective properties can be obtained by comparison

$$\sigma_{eff} = \sigma_1 \frac{1}{1 + \frac{cd\alpha_B}{(1-c)\alpha_C + c[\alpha_C - (d-1)\alpha_B]}}, \quad (38)$$

$$\chi_{eff} = \frac{\alpha_B\beta_C - \alpha_C\beta_B}{(\alpha_C + c\alpha_B)^4} cd^3 \sigma_1^3, \quad (39)$$

$$\delta_{eff} = -3\frac{(\beta_C + c\beta_B)(\alpha_B\beta_C - \alpha_C\beta_B)}{(\alpha_C + c\alpha_B)^7} cd^5 \sigma_1^5. \quad (40)$$

These expressions represent the main achievement of this section and will be used to analyze some particular cases, and to investigate the dependence of the nonlinear response upon the size of dispersed inhomogeneities (scale effects). We remark that we have developed a nonlinear generalization of the Maxwell approach⁴² or the Mori-Tanaka scheme⁴³ for obtaining simple results directly applicable to investigate the scale effects. Of course, other homogenization techniques could be applied as well: the differential method,⁴⁴⁻⁴⁶ the self consistent scheme,⁴⁷⁻⁴⁹ and the strong-property-fluctuation theory.⁵⁰

A. Perfect interfaces

If we consider a perfect contact between the constituents we obtain the celebrated Maxwell formula⁴² for the linear response and two expressions for the nonlinear coefficients, which are in perfect agreement with previous literature^{4,11}

$$\sigma_{max} = \sigma_1 \frac{1}{1 + \frac{dc(\sigma_1 - \sigma_2)}{(1-c)[(d-1)\sigma_1 + \sigma_2] + cd\sigma_2}}, \quad (41)$$

$$\chi_{max} = \frac{cd^4 \sigma_1^4 \chi_2}{[(d-1+c)\sigma_1 + (1-c)\sigma_2]^4}, \quad (42)$$

$$\delta_{max} = -3\frac{c(1-c)d^6 \sigma_1^6 \chi_2^2}{[(d-1+c)\sigma_1 + (1-c)\sigma_2]^7}. \quad (43)$$

It is interesting to notice that the term δ_{max} does not affect the nonlinear behavior for $c=0$ nor $c=1$, as expected. In our context, these results represent a simple check of the proposed procedure. Moreover, we also remark that in case of perfect interfaces the effective response is not influenced by the particle size and, therefore, no scale effects are observable.

B. Low-conducting interfaces

In order to obtain the linear and nonlinear results for the low conducting interface, we use the Π -model (Eqs. (31)–(34) combined to Eqs. (38)–(40)) with $g^+ = g^- = 0$. In this way, only the longitudinal resistivity r controls the properties of the interface. The explicit final results describing the linear and nonlinear effective parameters follow:

$$\sigma_{low} = \sigma_1 \frac{1}{1 + \frac{dc\left(\sigma_1 - \sigma_2 + \frac{r}{R}\sigma_1\sigma_2\right)}{(1-c)\left[(d-1)\sigma_1 + \sigma_2 + (d-1)\frac{r}{R}\sigma_1\sigma_2\right] + cd\sigma_2}}, \quad (44)$$

$$\chi_{low} = \frac{cd^4 \sigma_1^4 \chi_2}{\left[(d-1+c)\sigma_1\left(1 + \frac{r}{R}\sigma_2\right) + (1-c)\sigma_2\right]^4}, \quad (45)$$

$$\delta_{low} = -3\frac{cd^6 \sigma_1^6 \chi_2^2 \left[(1-c) + \frac{r}{R}\sigma_1(d-1+c)\right]}{\left[(d-1+c)\sigma_1\left(1 + \frac{r}{R}\sigma_2\right) + (1-c)\sigma_2\right]^7}. \quad (46)$$

We note that the expression for σ_{low} is in perfect agreement with recent investigations.^{26,27,33} In addition, the analysis of the scale effects describing the behavior of the linear conductivity σ_{low} can be found in Ref. 37. However, the expressions obtained for χ_{low} and δ_{low} are important for understanding the scale effects induced by the interfaces on the effective nonlinear behavior. It is evident that for a very large radius of the particles ($R \rightarrow \infty$) we have $\chi_{low} \rightarrow \chi_{max}$ and $\delta_{low} \rightarrow \delta_{max}$ and, therefore, the scale effects disappear for macroscopic systems. The scaling laws of the effective nonlinear properties can be formulated through the following developments:

$$\frac{\chi_{low}}{\chi_{max}} - 1 = -4\frac{1}{1 + \frac{\sigma_2}{\sigma_1} \frac{1-c}{d-1+c}} \frac{\ell}{R} + O\left(\frac{1}{R^2}\right), \quad (47)$$

$$\frac{\delta_{low}}{\delta_{max}} - 1 = \frac{-6 + \frac{\sigma_1}{\sigma_2} \frac{d-1+c}{1-c}}{1 + \frac{\sigma_2}{\sigma_1} \frac{1-c}{d-1+c}} \frac{\ell}{R} + O\left(\frac{1}{R^2}\right). \quad (48)$$

It is important to remark that ℓ in Eqs. (47) and (48) is the length scale defined in Eq. (14), also controlling the scaling laws of the electric field induced inside each particle and the scaling laws of the linear effective properties.³⁷ We also underline that Eqs. (47) and (48) mean that the effective nonlinear properties approach those of the Maxwell assemblage

for $R \gg \ell$, i.e., we quantitatively determined the crossover between the different length scales. For going towards the nanoscale we can now introduce the scaling laws describing the behavior of the system for $R \rightarrow 0$. A long but straightforward analysis leads to

$$\chi_{low} = \frac{\chi_2 c d^4}{(d-1+c)^4} \left(\frac{R}{\ell}\right)^4 + O(R^5), \quad (49)$$

$$\delta_{low} = \frac{-3 \chi_2^2 c d^6}{\sigma_2 (d-1+c)^6} \left(\frac{R}{\ell}\right)^6 + O(R^7). \quad (50)$$

In both cases, the nonlinear features converge to zero for very small particles. It is interesting to observe that χ_{low} follows a scaling law with a power of fourth degree, while δ_{low} follows a law with a scaling exponent equal to six.

C. High-conducting interfaces

A similar analysis has been conducted to understand the effects of the high conducting interfaces. This model can be simply obtained by using the T-structure (Eqs. (27)–(30) substituted into Eqs. (38)–(40)) with $r^+ = r^- = 0$. Therefore, the only parameter describing the behavior of the resulting interface is the transversal conductivity g . The linear and non-linear effective properties have been eventually found as

$$\sigma_{high} = \sigma_1 \frac{1}{1 + \frac{dc \left(\sigma_1 - \sigma_2 - \frac{d-1}{R} g \right)}{(1-c) \left[(d-1)\sigma_1 + \sigma_2 + \frac{d-1}{R} g \right] + cd \left(\sigma_2 + \frac{d-1}{R} g \right)}}, \quad (51)$$

$$\chi_{high} = \frac{cd^4 \sigma_1^4 \chi_2}{\left[(d-1+c)\sigma_1 + (1-c)\sigma_2 + (1-c)(d-1) \frac{g}{R} \right]^4}, \quad (52)$$

$$\delta_{high} = -3 \frac{c(1-c)d^6 \sigma_1^6 \chi_2^2}{\left[(d-1+c)\sigma_1 + (1-c)\sigma_2 + (1-c)(d-1) \frac{g}{R} \right]^7}. \quad (53)$$

First, we observe that the result for the linear conductivity σ_{high} perfectly corresponds to recent achievements.^{26,32,33} The scaling laws concerning such a parameter σ_{high} have been largely discussed in Ref. 37 and, therefore, we are now interested in analyzing the nonlinear effective response. As before, we remark that χ_{high} and δ_{high} are strongly size dependent and, for $R \rightarrow \infty$, they converge to the Maxwell counterparts given in Eqs. (42) and (43): $\chi_{high} \rightarrow \chi_{max}$ and $\delta_{high} \rightarrow \delta_{max}$. This convergence is described by the following scaling laws:

$$\frac{\chi_{high}}{\chi_{max}} - 1 = -4 \frac{\frac{(d-1)(1-c)}{d-1+c} \frac{\mathcal{L}}{R}}{1 + \frac{\sigma_2}{\sigma_1} \frac{1-c}{d-1+c}} + O\left(\frac{1}{R^2}\right), \quad (54)$$

$$\frac{\delta_{high}}{\delta_{max}} - 1 = -7 \frac{\frac{(d-1)(1-c)}{d-1+c} \frac{\mathcal{L}}{R}}{1 + \frac{\sigma_2}{\sigma_1} \frac{1-c}{d-1+c}} + O\left(\frac{1}{R^2}\right), \quad (55)$$

which are completely controlled by the length scale \mathcal{L} defined in Eq. (10). Previous results have been obtained by developing the quantity on the left hand sides in series of the variable $1/R$. To conclude the present discussion, we can also determine the behavior of the nonlinear properties for $R \rightarrow 0$. An accurate analysis proves that

$$\chi_{high} = \frac{\chi_2 c d^4}{(d+c-cd-1)^4} \left(\frac{R}{\mathcal{L}}\right)^4 + O(R^5), \quad (56)$$

$$\delta_{high} = \frac{-3 \chi_2^2 c d^6}{\sigma_1 (d-1)(d+c-cd-1)^6} \left(\frac{R}{\mathcal{L}}\right)^7 + O(R^8). \quad (57)$$

Interestingly, we note that χ_{high} and δ_{high} for $R \rightarrow 0$ are controlled by the scaling exponents four and seven, respectively. These values should be compared with those concerning the low conducting interface model: indeed, for χ_{low} and δ_{low} we got the scaling exponents four and six, respectively. Therefore, we can underline a different scaling behavior of the effective parameter δ_{eff} passing from the low to the high interface model.

D. T-model

We can now take into consideration the complete T-model described by the interface parameters r^+ , g , and r^- . Since the scaling laws concerning the linear conductivity σ_{eff}^T have been largely discussed in our previous work,³⁷ here we focus our attention on the nonlinear properties χ_{eff}^T and δ_{eff}^T : their scaling laws for $R \rightarrow \infty$ have been eventually found as

$$\frac{\chi_{eff}^T}{\chi_{max}^T} - 1 = -4 \frac{1}{1 + \frac{\sigma_2}{\sigma_1} \frac{1-c}{d-1+c}} \frac{\mathfrak{Q}_\chi^T}{R} + O\left(\frac{1}{R^2}\right), \quad (58)$$

$$\mathfrak{Q}_\chi^T = \ell^+ + \ell^- + \frac{(d-1)(1-c)}{d-1+c} \mathcal{L}, \quad (59)$$

$$\frac{\delta_{eff}^T}{\delta_{max}^T} - 1 = \frac{1}{1 + \frac{\sigma_2}{\sigma_1} \frac{1-c}{d-1+c}} \frac{\mathfrak{Q}_\delta^T}{R} + O\left(\frac{1}{R^2}\right), \quad (60)$$

$$\mathfrak{Q}_\delta^T = \left(-6 + \frac{\sigma_1}{\sigma_2} \frac{d-1+c}{1-c} \right) (\ell^+ + \ell^-) - 7 \frac{(d-1)(1-c)}{d-1+c} \mathcal{L}. \quad (61)$$

Once again, we remark that the scaling behavior of the effective nonlinear response is completely controlled by the three length scales ℓ^+ , ℓ^- , and \mathcal{L} , defined in Eq. (10) and already describing the linear scaling.³⁷ In fact, the characteristic length scales \mathfrak{Q}_χ^T and \mathfrak{Q}_δ^T are simply linear combinations of the three length scales above. Also the scaling laws obtained for $R \rightarrow 0$ can be interesting to understand the behavior of the system at the nanoscale. The obtained results follow:

$$\chi_{eff}^T = \frac{\chi_2 c d^4}{(d-1)^4 (d-1+c)^4} \left(\frac{\sigma_2}{\sigma_1} \right)^4 \left(\frac{R^3}{\ell^- \ell^+ \mathcal{L}} \right)^4 + O(R^{13}), \quad (62)$$

$$\delta_{eff}^T = \frac{-3 \chi_2^2 c d^6}{(d-1)^6 (d-1+c)^6} \left(\frac{\sigma_2}{\sigma_1} \right)^6 \left(\frac{R^3}{\ell^- \ell^+ \mathcal{L}} \right)^6 + O(R^{19}). \quad (63)$$

In this case, the scaling exponents are exactly three times those found previously for the low conducting interface model. This point can be related to the fact that the T-model may be interpreted through a series of three different layers (see Ref. 37 for details).

E. II-model

To complete our analysis we finally take into consideration the II-model described by the interface parameters g^+ , r , and g^- . As before, we discuss only the nonlinear properties, since the linear ones have been largely explained in previous literature.³⁷ We determine χ_{eff}^T and δ_{eff}^T through Eqs. (39) and (40) and we analyze their scaling laws for $R \rightarrow \infty$: with long but straightforward calculations we eventually found the following results:

$$\frac{\chi_{eff}^{\Pi}}{\chi_{max}} - 1 = -4 \frac{1}{1 + \frac{\sigma_2}{\sigma_1} \frac{1-c}{d-1+c}} \frac{\mathcal{Q}_\lambda^{\Pi}}{R} + O\left(\frac{1}{R^2}\right), \quad (64)$$

$$\mathcal{Q}_\lambda^{\Pi} = \ell + \frac{(d-1)(1-c)}{d-1+c} (\mathcal{L}^- + \mathcal{L}^+), \quad (65)$$

$$\frac{\delta_{eff}^{\Pi}}{\delta_{max}} - 1 = \frac{1}{1 + \frac{\sigma_2}{\sigma_1} \frac{1-c}{d-1+c}} \frac{\mathcal{Q}_\delta^{\Pi}}{R} + O\left(\frac{1}{R^2}\right), \quad (66)$$

$$\mathcal{Q}_\delta^{\Pi} = \left(-6 + \frac{\sigma_1 d - 1 + c}{\sigma_2} \right) \ell - 7 \frac{(d-1)(1-c)}{d-1+c} (\mathcal{L}^- + \mathcal{L}^+). \quad (67)$$

As before, we observe that the scaling behavior of the effective nonlinear response is controlled by $\mathcal{Q}_\lambda^{\Pi}$ and \mathcal{Q}_δ^{Π} , which are linear combinations of the three length scales \mathcal{L}^+ , \mathcal{L}^- , and ℓ , defined in Eq. (14) and already describing the linear scaling.³⁷ The scaling laws obtained for $R \rightarrow 0$ can be useful to understand the behavior of the system at the nanoscale

$$\chi_{eff}^{\Pi} = \frac{\chi_2 c d^4}{(d-1)^8 (1-c)^4} \left(\frac{\sigma_2}{\sigma_1} \right)^4 \left(\frac{R^3}{\ell \mathcal{L}^- \mathcal{L}^+} \right)^4 + O(R^{13}), \quad (68)$$

$$\delta_{eff}^{\Pi} = \frac{-3 \chi_2^2 c d^6}{(d-1)^{13} (1-c)^6} \left(\frac{\sigma_2}{\sigma_1} \right)^7 \frac{R}{\mathcal{L}^-} \left(\frac{R^3}{\ell \mathcal{L}^- \mathcal{L}^+} \right)^6 + O(R^{20}). \quad (69)$$

As before, we note that the scaling exponent of χ_{eff}^{Π} is identical to that of χ_{eff}^T . On the contrary, the exponent of δ_{eff}^{Π} is larger than the exponent of δ_{eff}^T . A similar situation was described at the end of Sec. IV C.

F. Results and discussion

In Figs. 2 and 3 one can find the results for a three dimensional dispersion with a fixed volume fraction $c = 0.3$ and a varying radius of the particles. The linear (σ_{eff}) and nonlinear (χ_{eff} and δ_{eff}) parameters are shown versus $\log_{10} R$. The plots correspond to the case $\sigma_2 > \sigma_1$ (Fig. 2) and $\sigma_1 > \sigma_2$ (Fig. 3). In both cases we adopted $\chi_2 = 1$ and we considered all possible imperfect interfaces. The parameters σ_0 and σ_∞ exploited in the first panel of Figs. 2 and 3 represent the conductivity of a dispersion of voids and of superconducting particles, respectively, (see Ref. 37 for details). For the linear response we observe that for low and high conducting interfaces the scale effects are described by

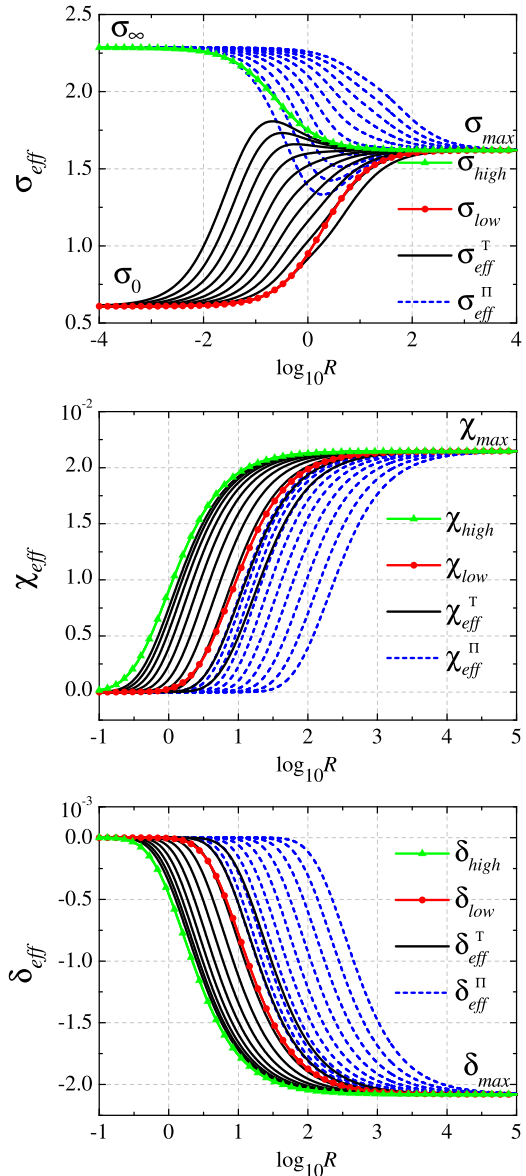


FIG. 2. Results for a material ($d=3$, $c=0.3$) composed of two homogeneous media with $\sigma_1 = 1$, $\sigma_2 = 5$, and $\chi_2 = 1$ (a.u.). For the high conducting interface (green lines with triangles), we used $g = 1$; for the low conducting interface (red lined with circles), we used $r = 1$; for the T-model (continuous black lines), we added $1/100 < r^+ = r^- < 1$ (ten values) to the high conducting interface; finally for the II-model (dashed blue lines), we added $1 < g^+ = g^- < 100$ (ten values) to the low conducting interface. The effective responses are shown in terms of $\log_{10} R$.

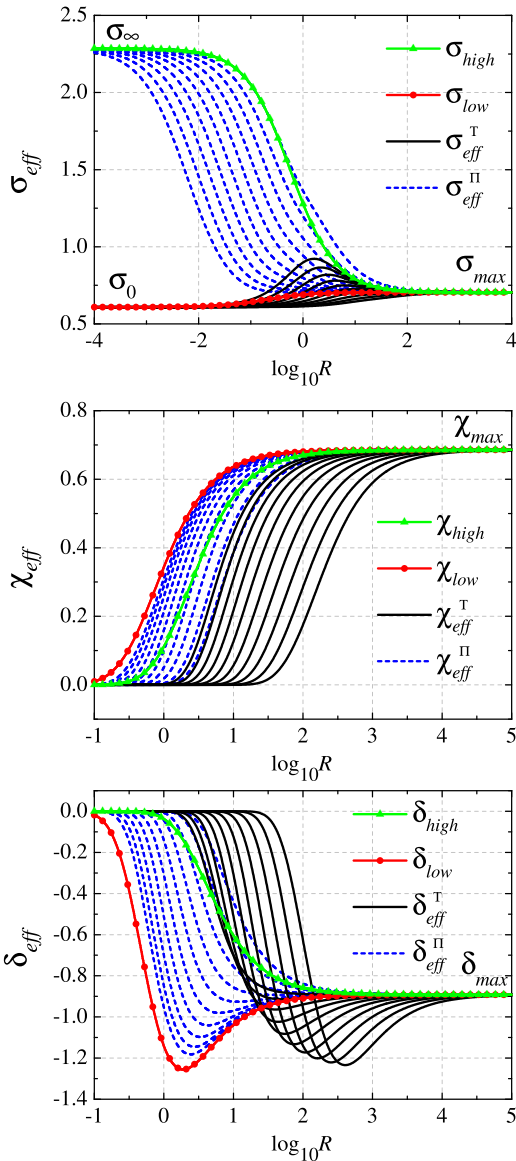


FIG. 3. Results for a material ($d=3$, $c=0.3$) composed of two homogeneous media with $\sigma_1 = 1$, $\sigma_2 = 1/5$, and $\chi_2 = 1$ (a.u.). For the high conducting interface (green lines with triangles), we used $g=1$; for the low conducting interface (red lined with circles), we used $r=1$; for the T-model (continuous black lines), we added $1 < r^+ = r^- < 100$ (ten values) to the high conducting interface; finally for the Π -model (dashed blue lines), we added $1/100 < g^+ = g^- < 1$ (ten values) to the low conducting interface. The effective responses are shown in terms of $\log_{10} R$.

monotone scaling law; on the contrary, the T and Π models show non-monotone scale effects with quite large peaks of the transport properties. This behavior has been recently observed in a dispersion of SiC particles (with radius between 5 and 15 Å) embedded in a polymeric (epoxy) matrix.⁵¹ These results are in qualitative agreement with our T-model. However, the linear behavior of the generalized interfaces is widely discussed in Ref. 37 and, therefore, we are here more interested in the nonlinear scaling. The results for χ_{eff} show that we always have monotone scale effects for the first nonlinear coefficient. In fact, with different interface behaviors we obtain different crossovers between the scales (identified by the inflection point of each curve) but in any case we observe an increasing value of χ_{eff} starting from

zero (for infinitesimal particles) and reaching χ_{max} for a large radius of the particles. Concerning the nonlinear coefficient δ_{eff} , we observe a different behavior. For the high conducting interface we have a monotone scaling in any case; for the low conducting interface we can observe a non-monotone behavior if $-6 + \frac{\sigma_1 d - 1 + c}{\sigma_2 (1 - c)} > 0$ (see Eq. (48)); this condition is e.g., satisfied in Fig. 3). For the T-model or the Π -model, we find a non-monotone behavior if $\Omega_{\delta}^T > 0$ or $\Omega_{\delta}^{\Pi} > 0$, respectively (see Eqs.(60) and (66)). Examples of peaks corresponding to the latter case are reported in the third panel of Fig. 3. Finally, for some combinations of parameters and for particular imperfect interfaces, the nonlinear scaling response can show pronounced peaks, which can be interesting for designing materials with desired and controlled strong nonlinear properties.

V. SUMMARY AND CONCLUSIONS

In this paper, we have analyzed the scale effects induced by imperfect interfaces on the effective nonlinear behavior of nanocomposites. To this aim we considered a paradigmatic system composed of nonlinear particles embedded in a linear matrix through imperfect interfaces. At the beginning, we considered an arbitrary nonlinearity of the particles and afterwards, to obtain concrete results, we applied the general procedure to the case of Kerr-like nonlinearities. To join inclusions and matrix we used two interface schemes, namely the T and Π structures, recently introduced to generalize the classical low and high conducting interfaces. The obtained results describe the scale effects of the nonlinear properties of the overall system: it means that we studied how the size of the particle affects the nonlinear effective response, especially at the nanoscale, which is pertinent to many composite of technological interest. The main achievements can be summarized as follows:

- The scaling laws for $R \rightarrow \infty$ are always described by a scaling exponent equal to one (dependence $1/R$) for both the linear and nonlinear properties. This value can be explained in terms of the sole competition between surface and volume effects. The different models for the imperfect interfaces can only affect the value of the overall length scale, which however is in any case the linear combination of certain intrinsic length scales defined in Sec. III.
- Differently, the scaling laws for $R \rightarrow 0$ exhibit some scaling exponents strongly depending on the situation taken into account. These exponents depend on the parameter considered (σ_{eff} , χ_{eff} , or δ_{eff}), and they increase with the degree of nonlinearity of the effective parameter. Moreover, they also depend on the kind of imperfect interface considered, being again increasing with the level of complexity of the model. This point can be explained by observing that the most complicated models (T or Π) can be obtained by a multilayered structure composed of simpler models (low and high conducting interfaces). Finally, as before all scaling laws can be described by the same intrinsic length scales defined in Sec. III.

We remark that throughout the paper we developed the formalism in the context of the electrical transport, but all

results can be applied to the analogous situations of thermal conduction, antiplane elasticity, magnetic permeability, and electric permittivity as well.

ACKNOWLEDGEMENTS

F.P. acknowledges financial support from the Seventh Framework Program for Research of the European Commission FP7/2007-2013 (Grant agreement 238393).

- ¹S. Torquato, *Random Heterogeneous Materials* (Springer-Verlag, New York, 2002).
- ²G. W. Milton, *The Theory of Composites* (Cambridge University Press, Cambridge, 2002).
- ³L. D. Landau and E. M. Lifshitz, *Electrodynamics of Continuous Media* (Pergamon Press, London, 1984).
- ⁴K. W. Yu, P. M. Hui, and D. Stroud, *Phys. Rev. B* **47**, 14150 (1993).
- ⁵K. W. Yu, Y. C. Wang, P. M. Hui, and G. Q. Gu, *Phys. Rev. B* **47**, 1782 (1993).
- ⁶K. W. Yu and G. Q. Gu, *Phys. Rev. B* **47**, 7568 (1993).
- ⁷D. J. Bergman, O. Levy, and D. Stroud, *Phys. Rev. B* **49**, 129 (1994).
- ⁸O. Levy, D. J. Bergman, and D. Stroud, *Phys. Rev. E* **52**, 3184 (1995).
- ⁹P. M. Hui, P. Cheung, and D. Stroud, *J. Appl. Phys.* **84**, 3451 (1998).
- ¹⁰P. M. Hui, C. Xu, and D. Stroud, *Phys. Rev. B* **69**, 014203 (2004).
- ¹¹S. Giordano and W. Rocchia, *J. Appl. Phys.* **98**, 104101 (2005).
- ¹²S. Giordano, *Materials* **2**, 1417 (2009).
- ¹³S. Giordano, *J. Electrostat.* **68**, 227 (2010).
- ¹⁴A. V. Goncharenko, V. V. Popelnukh, and E. F. Venger, *J. Phys. D: Appl. Phys.* **35**, 1833 (2002).
- ¹⁵E.-B. Wei and Z.-K. Wu, *J. Phys. Condens. Matter* **16**, 5377 (2004).
- ¹⁶P. L. Kapitza, *Collected Papers of P. L. Kapitza* (Pergamon Press, Oxford, 1964-1967), Vol. 3.
- ¹⁷Y. Benveniste and T. Miloh, *Int. J. Eng. Sci.* **24**, 1537 (1986).
- ¹⁸Y. Benveniste, *J. Appl. Phys.* **61**, 2840 (1987).
- ¹⁹D. P. H. Hasselman and L. F. Johnson, *J. Compos. Mater.* **21**, 508 (1987).
- ²⁰S. Torquato and M. D. Rintoul, *Phys. Rev. Lett.* **75**, 4067 (1995).
- ²¹R. Lipton and B. Vernescu, *Proc. R. Soc. London, Ser. A* **452**, 329 (1996).
- ²²R. Lipton and B. Vernescu, *J. Appl. Phys.* **79**, 8964 (1996).
- ²³H. Cheng and S. Torquato, *Proc. R. Soc. London, Ser. A* **453**, 145 (1997).
- ²⁴C.-W. Nan, R. Birringer, D. R. Clarke, and H. Gleiter, *J. Appl. Phys.* **81**, 6692 (1997).
- ²⁵Z. Hashin, *J. Appl. Phys.* **89**, 2261 (2001).
- ²⁶H. L. Duan and B. L. Karihaloo, *Phys. Rev. B* **75**, 064206 (2007).
- ²⁷H. Le Quang, Q.-C. He, and G. Bonnet, *Philos. Mag.* **91**, 3358 (2011).
- ²⁸R. Lipton, *SIAM J. Appl. Math.* **57**, 347 (1997).
- ²⁹R. Lipton, *J. Mech. Phys. Solids* **45**, 361 (1997).
- ³⁰T. Miloh and Y. Benveniste, *Proc. R. Soc. London, Ser. A* **455**, 2687 (1999).
- ³¹J. Yvonnet, Q.-C. He, and C. Toulemonde, *Compos. Sci. Technol.* **68**, 2818 (2008).
- ³²H. Le Quang, G. Bonnet, and Q.-C. He, *Phys. Rev. B* **81**, 064203 (2010).
- ³³H. Le Quang, D. C. Pham, G. Bonnet, and Q.-C. He, *Int. J. Heat Mass Transfer* **58**, 175 (2013).
- ³⁴Y. Benveniste, *J. Mech. Phys. Solids* **54**, 708 (2006).
- ³⁵Y. Benveniste, *Proc. R. Soc. London, Ser. A* **462**, 1593 (2006).
- ³⁶S. T. Gu and Q. C. He, *J. Mech. Phys. Solids* **59**, 1413 (2011).
- ³⁷F. Pavanello, F. Manca, P. L. Palla, and S. Giordano, *J. Appl. Phys.* **112**, 084306 (2012).
- ³⁸H. Hatta and M. Taya, *J. Appl. Phys.* **58**, 2478 (1985).
- ³⁹W. S. Weiglhofer, A. Lakhtakia, and B. Michel, *Microwave Opt. Technol. Lett.* **15**, 263 (1997).
- ⁴⁰S. Giordano and P. L. Palla, *J. Phys. A: Math. Theor.* **41**, 415205 (2008).
- ⁴¹L. Colombo and S. Giordano, *Rep. Prog. Phys.* **74**, 116501 (2011).
- ⁴²J. C. Maxwell, *A Treatise on Electricity and Magnetism* (Clarendon Press, Oxford, 1881).
- ⁴³T. Mori and K. Tanaka, *Acta Metall.* **21**, 571 (1973).
- ⁴⁴S. Giordano, *J. Electrostat.* **58**, 59 (2003).
- ⁴⁵B. Michel, A. Lakhtakia, W. S. Weiglhofer, and T. G. Mackay, *Compos. Sci. Technol.* **61**, 13 (2001).
- ⁴⁶S. Giordano and P. L. Palla, *Eur. Phys. J. B* **85**, 59 (2012).
- ⁴⁷A. Lakhtakia, *Microwave Opt. Technol. Lett.* **17**, 276 (1998).
- ⁴⁸S. Giordano, *Int. J. Circuit. Theory Appl.* **33**, 519 (2005).
- ⁴⁹S. Giordano, *Physica A* **375**, 726 (2007).
- ⁵⁰T. G. Mackay, *J. Nanophotonics* **5**, 051001 (2011).
- ⁵¹S. Yu, S. Yang, and M. Cho, *J. Appl. Phys.* **110**, 124302 (2011).